DNA binding, photocleavage behavior, and topoisomerase I inhibitory activity of Ru(II) complexes incorporating an asymmetric phenazine-type ligand

Xue-Wen Liu, Jun-Shi Shu, Yang Xiao, You-Ming Shen, Song-Bai Zhang & Ji-Lin Lu

View supplementary material 🗗

Accepted author version posted online: 05 Jun 2015.
Published online: 25 Jun 2015.

Submit your article to this journal 🗗

Article views: 55

View related articles 🗗

View Crossmark data 🗗

Taylor & Francis
Taylor & Francis Group

DNA binding, photocleavage behavior, and topoisomerase I inhibitory activity of Ru(II) complexes incorporating an asymmetric phenazine-type ligand

XUE-WEN LIU*, JUN-SHI SHU, YANG XIAO, YOU-MING SHEN,
SONG-BAI ZHANG and JI-LIN LU

College of Chemistry and Chemical Engineering, Hunan University of Arts and Science, ChangDe,
PR China
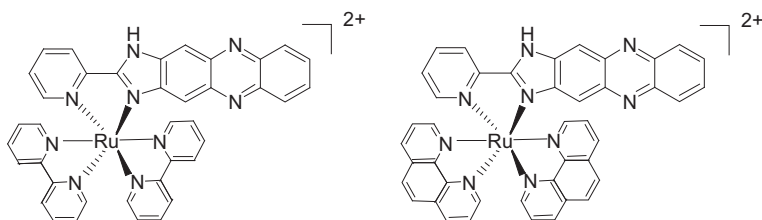
Two ruthenium complexes incorporating an asymmetric ligand, $[Ru(L)_2pipz]^{2+}$ (L = bpy (2,2′-bipyridine), phen (1,10-phenanthroline), pipz = 2-pyridine-1H-imidazo[4,5-b]phenazine), have been synthesized and characterized. The interactions of the two complexes with DNA have been investigated by UV–visible spectroscopy, fluorescence spectroscopy, and viscosity measurements. Both complexes bind to DNA by intercalation and efficiently cleave pBR322 DNA under irradiation. Singlet oxygen ($^1O_2$) was the main reactive oxygen species involved in DNA photocleavage. Topoisomerase inhibition and DNA strand passage assay demonstrated that both complexes can act as efficient catalytic inhibitors of DNA topoisomerase I.

1. Introduction

There has been interest in the interaction of small molecules with DNA, as DNA is a key target for widely used anticancer drugs such as intercalators and platinum drugs, which are generally believed to interact primarily with duplex DNA [1]. Small molecules can bind to DNA through covalent and non-covalent interactions. Covalent interactions result in adduct formation and a permanent change to DNA as a result of new bonds being formed as found for cisplatin [2–5]. Non-covalent interactions include intercalation, minor groove DNA

---

*Corresponding author. Email: liuxuewen050@sina.com

binding, major groove DNA binding, and electrostatic interactions, which are reversible processes [6, 7]. Among small molecules, mononuclear Ru(II) complexes with polypyridine ligands have been widely investigated due to their special DNA binding behaviors and possible applications as nucleic acid probes [8–11], DNA molecular "light switches" [12–15], photodynamic therapy (PDT) agents [16–18], topoisomerase inhibitors [19–25], chemotherapeutics [26–35], and diagnostic and imaging probes [36–39]. Of these, DNA molecular "light switches" is one of the hot applications for mononuclear Ru(II) complexes, owing to their possible applications such as in the detection of DNA base mismatches [40], molecular-scale logic gates, DNA sensing, signaling of DNA–protein binding [41–44], and as luminescent probes of DNA structure. Previous research has shown that mononuclear Ru(II) complexes containing dppz-based ligands behave as DNA molecular "light switches" through various modes, such as "off-on" light switches based on DNA binding (as observed for $[Ru(bpy)_2(dppz)]^{2+}$ (bpy = 2,2′-bipyridine; dppz = dipyrido[3,2-*a*:2′,3′-*c*]phenazine)) [14], and repeated switching of the DNA light switch between the on and off positions by the addition of metal ions (off) followed by EDTA (on) (observed for $[Ru(bpy)_2(tpphz)]^{2+}$ (tpphz = tetrapyrido[3,2-*a*:2′,3′-*c*:3″,2″-*h*:2‴,3‴-*j*]phenazine)) [45, 46]. These dppz-based ligands usually possess a phenazine ring, and protection of the phenazine nitrogen from solvent molecules appears to be a requirement for ruthenium light switch complexes in DNA solutions. In recent years, ruthenium complexes containing a phenazine ring have been designed to act as DNA molecular "light switches," such as $[Ru(phen)_2dppz-idzo]^{2+}$ and $[Ru(bpy)_2(pidbp))]^{2+}$ [47, 48]. The emission quenching in water arises from the formation of hydrogen bonds between water and the phenazine N of the ruthenium(II) complexes, which stabilize the low-lying Ru dppz metal-to-ligand charge transfer triplet-excited state [45]. The presence of DNA prevents the formation of hydrogen bonds, which leads to the emission recovery.

Ruthenium complexes with a wide range of ligands have been designed to investigate their binding to DNA due to their diverse photochemical properties. Ru(II) complexes which intercalate to DNA can incorporate either symmetric or asymmetric ligands. Previous studies show that modifying the structure of the intercalative ligand of the Ru(II) complex modulates the DNA-binding mode, the DNA-binding affinity, and/or the photocleavage properties [47–51]. Thus, the development of Ru(II) complexes incorporating intercalative ligands shows much promise.

Recently DNA topoisomerase I inhibitors have attracted attention as antitumor agents since DNA topoisomerase I (Topo I) is an important enzyme found in the nucleus that regulates the topological state of DNA during many cellular processes such as replication, transcription, recombination, and chromosome segregation at mitosis [52–54]. A number of compounds have been developed as Topo I inhibitors. Amongst these compounds, Ru(II) polypyridyl complexes have attracted considerable attention as topoisomerase I inhibitors [19–25, 55, 56]. However, the vast majority of these studies have been primarily focused on symmetric intercalative ligands, with Ru(II) complexes incorporating asymmetric ligands attracting much less attention.

Herein, ruthenium complexes incorporating an asymmetric phenazine ligand (pipz = 2-pyridine-1H-imidazo[4,5-b]phenazine), $[Ru(L)_2(pipz)]^{2+}$ (L = bpy (2,2′-bipyridine) or phen (1,10-phenanthroline)), have been synthesized (scheme 1) and characterized. The DNA binding, DNA photocleavage properties, and topoisomerase I inhibitory activities of the two Ru(II) complexes have also been studied.
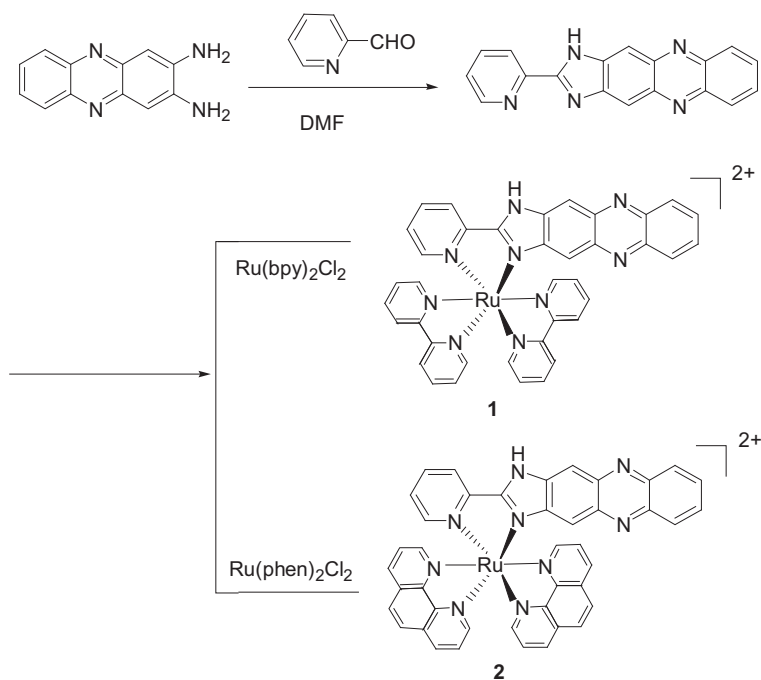
Scheme 1. The synthetic routes of $[Ru(bpy)_2(pipz)]^{2+}$ (**1**) and $Ru(phen)_2(pipz)]^{2+}$ (**2**).

2. Experimental

2.1. *Materials*

cis-[Ru(bpy)$_2$Cl$_2$]·2H$_2$O, *cis*-[Ru(phen)$_2$Cl$_2$]·2H$_2$O [57], 2,3-diamino-phenazine, and 2-pyridine-1H-imidazo[4,5-b]phenazine (pipz) [58] were prepared following literature procedures. Calf thymus (CT) DNA (CT-DNA) was purchased from Sigma (USA). Supercoiled pBR 322 DNA was obtained from MBI Fermentas and applied to DNA photocleavage and topoisomerase inhibition. DNA topoisomerase I from CT was obtained from Takara. All buffer solutions were prepared using deionized water as follows: (i) buffer A (50 mM NaCl, 5 mM Tris-HCl, pH 7.2); (ii) buffer B (50 mM Tris, 18 mM NaCl, pH 7.8); (iii) buffer C (89 mM Tris, 89 mM boric acid, 2 mM EDTA); (iv) buffer D 50 mM Tris-HCl (pH 7.5), 72 mM KCl, 5 mM MgCl$_2$, 5 mM DTT, 2 mM sperdine, 0.1 mg mL^{-1} BSA.

2.2. *Physical measurements*

Microanalyses (C, H, and N) were determined on a Perkin–Elmer 240Q elemental analyzer. UV–vis spectra were recorded on a Shimadzu UV-2450 spectrophotometer and emission spectra were recorded on a Hitachi F-2500 spectrofluorophotometer at room temperature. ^{1}H NMR spectra of the complexes were recorded on a Bruker ARX-500 spectrometer with (CD$_3$)$_2$SO as the solvent at room temperature. Electrospray mass spectra were recorded on a LQC system (Finnigan MAT, USA) using CH$_3$CN as the mobile phase.

2.3. *Synthesis*

2.3.1. [Ru(bpy)$_2$(pipz)](ClO$_4$)$_2$. H$_2$O (1). 2-Pyridine-1H-imidazo[4,5-b]phenazine 0.090 g (*ca.* 0.3 mmol), [Ru(bpy)$_2$Cl$_2$] 0.156 g (0.3 mmol), and 10 mL ethylene glycol were heated at 120 °C under argon for 6 h, whereupon the color changed from dark purple to dark red. After cooling to room temperature, the solution was poured into 80 mL of water. The red–brown precipitate was obtained by addition of NaClO$_4$. The complex was purified by column chromatography on a neutral alumina column with acetonitrile–toluene (3 : 1, v/v) as an eluent. Yield: 0.126 g, 45.3%. Anal. (%): (Found: C, 49.10; H, 3.19; N, 13.55%. Calcd for C$_{38}$H$_{29}$N$_9$O$_9$RuCl$_2$: C, 49.19; H, 3.15; N, 13.59%). ES-MS (CH$_3$CN): m/z = 710.4 ([C$_{38}$H$_{29}$N$_9$O$_9$RuCl$_2$−2ClO$_4$$^-$-H]$^+$), 355.6 ([C$_{38}H_{29}N_9O_9$RuCl$_2$−2ClO$_4$$^-$]$^{2+}$). ^{1}H NMR (500 MHz, ppm, DMSO-d$_6$): 8.96 (d, 1H, J = 7.5 Hz), 8.88 (dd, 2H, J_1 = 9.0 Hz, J_2 = 8.5 Hz), 8.78 (d, 1H, J = 8.0 Hz), 8.69 (d, 1H, J = 7.5 Hz), 8.48 (s, 1H), 8.42 (t, 1H, J_1 = 8.0 Hz, J_2 = 7.5 Hz), 8.17 (m, 5H), 8.12 (t, 2H, J_1 = 8.5 Hz, J_2 = 7.0 Hz), 8.00 (d, 1H, J = 5.5 Hz), 7.93 (d, 3H, J = 5.5 Hz), 7.79 (m, 4H), 7.72 (d, 1H, J = 5.0 Hz), 7.61 (t, 1H, J_1 = 5.5 Hz, J_2 = 7.5 Hz), 7.58 (dd, 2H, J_1 = 6.0 Hz, J_2 = 6.0 Hz), 7.49 (t, 1H, J_1 = 7.0 Hz, J_2 = 7.5 Hz), 6.40 (s, 1H).

2.3.2. [Ru(phen)$_2$(pipz)](ClO$_4$)$_2$·H$_2$O (2). This complex was synthesized using a similar method as described for **1**, but with [Ru(phen)$_2$Cl$_2$] 0.170 g (0.3 mmol) in place of [Ru(bpy)$_2$Cl$_2$]. Yield: 0.106 g, 34.8%. Anal. (%): (Found: C, 51.61; H, 3.05; N, 12.88%. Calcd for C$_{42}$H$_{29}$N$_9$O$_9$RuCl$_2$: C, 51.69; H, 3.00; N, 12.93%). ES-MS (CH$_3$CN): m/z = 758.6 ([C$_{42}$H$_{29}$N$_9$O$_9$RuCl$_2$−2ClO$_4$$^-$-H]$^+$), 379.7 ([C$_{42}H_{29}N_9O_9$RuCl$_2$−2ClO$_4$$^-$]$^{2+}$). ^{1}H NMR (500 MHz, ppm, DMSO-d$_6$): 8.91 (d, 1H, J = 7.5 Hz), 8.73 (t, 2H, J_1 = 8.5 Hz, J_2 = 8.5 Hz), 8.66 (d, 2H, J = 8.0 Hz), 8.43 (d, 1H, J = 5.0 Hz), 8.39 (d, 1H, J = 2.5 Hz), 8.37 (s, 1H), 8.36 (s, 2H), 8.33 (d, 1H, J = 5.5 Hz), 8.29 (d, 1H, J = 8.5 Hz), 8.19 (d, 1H, J = 5.0 Hz), 8.12 (dd, 2H, J_1 = 4.0 Hz, J_2 = 7.5 Hz), 8.06 (d, 1H, J = 7.5 Hz), 7.91 (dd, 3H, J_1 = 5.5 Hz, J_2 = 5.5 Hz), 7.85 (dd, 1H, J_1 = 5.5 Hz, J_2 = 5.5 Hz), 7.75 (dd, 1H, J_1 = 5.5 Hz, J_2 = 5.0 Hz), 7.69 (t, 2H, J_1 = 7.5 Hz, J_2 = 6.5 Hz), 7.64 (d, 1H, J = 5.5 Hz), 7.38 (t, 1H, J_1 = 7.5 Hz, J_2 = 7.0 Hz), 6.07 (s, 1H).

2.4. *DNA binding and photocleavage experiments*

All experiments involving the binding of Ru(II) complexes with CT-DNA were carried out in buffer A. The solution of CT-DNA in buffer A gave a ratio of UV–vis absorbance of 1.8–1.9 : 1 at 260 and 280 nm, indicating that the DNA was sufficiently free of protein [59]. The concentration of DNA was determined using ε = 6,600 M^{-1} cm^{-1} at 260 nm [60].

In order to determine the DNA binding affinities and provide fundamental information for DNA-binding mode, absorption titration experiments were performed with fixed concentration of Ru(II) complexes (20 μM) in buffer A and varying DNA concentrations (0–400 μM). Ruthenium-DNA solutions (3 mL) were allowed to incubate for 5 min before the spectra were recorded. The intrinsic binding constants K of both ruthenium(II) complexes bound to DNA were calculated using equations (1a) and (1b) [61],

$$(\varepsilon_a - \varepsilon_f) / (\varepsilon_b - \varepsilon_f) = (b - (b^2 - 2K^2 C_t \,[\text{DNA}]/s)^{1/2})/2KC_t \qquad (1a)$$

$$b = 1 + KC_t + K \, [\text{DNA}]/2s \tag{1b}$$

where ε_a, ε_b, and ε_f are the extinction coefficient for the apparent, bound, and free Ru(II) complexes, K is the equilibrium binding constant in M^{-1}, C_t is the total metal complex concentration, [DNA] is the concentration of DNA in M (nucleotide), and s is the binding site size. The experimental absorption titration data were fitted to obtain the binding constants by a non-linear least-squares method.

The fluorescence titration experiments were carried out by keeping the concentration of the Ru(II) complexes constant (5 μM) while varying the DNA concentration from 0 to 150 μM. The samples were excited at 450 nm and emission spectra were recorded in the region 500–750 nm.

DNA viscosity experiments were carried using a Ubbelohde viscometer, maintained at 30.0 ± 0.1 °C using a thermostated bath. The DNA viscosity was calculated using $\eta_i = (t_i - t_0)/t_0$, where η_i is the DNA viscosity, t_i is the flow time of the solutions in the presence or absence of the complex, and t_0 is the flow time of the buffer alone. Data were presented as $(\eta/\eta_0)^{1/3}$ versus binding ratio [62], where η is the viscosity of DNA in the presence of complex and η_0 is the viscosity of DNA alone.

The concentration-dependent DNA photocleavage experiments for the Ru(II) complexes were carried out by treating supercoiled pBR322 DNA (0.1 μg) with varying concentrations of the Ru(II) complexes in buffer B. The mixed solutions were incubated for 1 h in the dark and then irradiated with an UV lamp (365 nm, 10 W) at room temperature. The reaction mixtures were loaded onto 1% agarose gel. Electrophoresis was performed for 2 h at 75 V in TBE buffer C. The gel was stained with $0.5 \, \mu\text{g mL}^{-1}$ ethidium bromide (EB) and photographed under UV light.

2.5. Quantum yield of $^1O_2$ generation

The quantum yields for $^1O_2$ generation from the Ru(II) complexes were determined using the reaction between 1,3-diphenylisobenzofuran (DPBF) and singlet oxygen. Air-saturated methanol solutions (2 mL) containing DPBF (20 μM) and the Ru(II) complex (20 μM) were irradiated at 450 nm (a Hitachi F-2500 spectrofluorophotometer was used with a 5 nm excitation slit width). The consumption of DPBF was determined by monitoring the decrease in fluorescence intensity at the emission maximum for DPBF ($\lambda_{ex} = 405$ nm, $\lambda_{em} = 479$ nm) at varying irradiation times.

The $^1O_2$ generation quantum yield (Φ_Δ) was calculated according to equations (2a) and (2b), where I_{in} is the incident monochromatic light intensity, Φ_{ab} is the light absorbing efficiency of the photosensitizer, Φ_r is the reaction quantum yield of $^1O_2$ with DPBF, t is the irradiation time, I_0 and I_t are the fluorescence intensity of DPBF before and after irradiation, respectively, k is the slope, and the superscript s stands for standard.

$$\frac{-\Delta[\text{DPBF}]}{t} = \frac{I_0 - I_t}{I_0} = I_{in}\Phi_{ab}\Phi_\Delta\Phi_r \tag{2a}$$

$$\frac{k}{k^s} = \frac{\Phi_{ab}}{\Phi_{ab}^s} = \frac{\Phi_\Delta}{\Phi_\Delta^s} \tag{2b}$$

2.6. *Topoisomerase I inhibition assay*

The abilities of the Ru(II) complexes to inhibit Topo I were determined by a DNA relaxation assay. The relaxation assay was performed in buffer D containing 0.1 μg pBR322 DNA and 1U Topo I. After incubation at 37 °C for 30 min (total volume = 10 μL), the reactions were quenched by the addition of 4 μL loading buffer (0.25% bromophenol blue, 4.5% sodium dodecyl sulfate, and 45% glycerol). Samples were subjected to electrophoresis using 1% agarose gel in buffer C as described in the section on DNA photocleavage. The concentrations of the inhibitor that prevented 50% of the supercoiled DNA from being converted into relaxed DNA (IC_{50} values) were calculated from the midpoint concentration for drug-induced DNA unwinding.

2.7. *DNA strand passage assay*

The DNA strand passage activity of topoisomerase I was examined by monitoring the ability of the enzyme to relax negatively supercoiled plasmid DNA in the absence of the Ru(II) complexes and the ability of the enzyme to supercoil relaxed plasmid substrates in the presence of 80 μM EB or the Ru(II) complexes. Reactions mixtures contained 0.3 μg pBR322 DNA and 5 U Topo I in buffer D (total volume = 40 μL). After a 5 min incubation of DNA with the drug, Topo I was added and the reaction mixtures were incubated for varying times at 37 °C. Reactions were stopped and subjected to electrophoresis as described above.

3. Results and discussion

3.1. *Electronic absorption titration*

Absorption titrations are one of the most useful ways to study the DNA binding properties of a complex. If metal complexes intercalate to DNA, hypochromism and a red shift (bathochromism) typically occurs, due to a strong π–π stacking interaction between the aromatic chromophore of the complex and the base pairs of DNA. The extent of the hypochromism in the visible ^{1}MLCT band is usually consistent with the intercalative binding strength [63].

Figure 1 shows UV–vis spectra of the complexes $[Ru(bpy)_2(pipz)]^{2+}$ and $Ru(phen)_2$ $(pipz)]^{2+}$ in the presence of increasing concentration of CT-DNA. By comparing with the UV–vis spectra of the ligand [58], the bands at 290 nm for **1** and 264 nm for **2** are assigned to bpy-centered and phen-centered π–π* transitions, respectively; the band of **2** at 294 nm is attributed to intraligand (IL) π–π* transitions of the pipz ligand. In the visible region, the bands at 412 nm for **1** and 413 nm for **2** are also attributed to IL π–π* transitions of pipz. The weak and broad MLCT absorption bands appear at 450–500 nm for both complexes. With increasing concentrations of CT-DNA, the UV–vis spectra of the two complexes showed clear hypochromism in the absorption bands. For **1**, upon addition of DNA, the band at 412 nm exhibits hypochromism of 23.9% at a ratio of [DNA]/[Ru] = 19.5. For **2**, the hypochromism at 413 nm reaches 29.5% at a ratio of [DNA]/[Ru] = 16.0. For both complexes, no obvious red shift was observed. The hypochromism induced by DNA binding suggests that both complexes bind to DNA with high affinity, and most likely through strong interaction between the aromatic chromophore of the two Ru(II) complexes and the DNA bases.
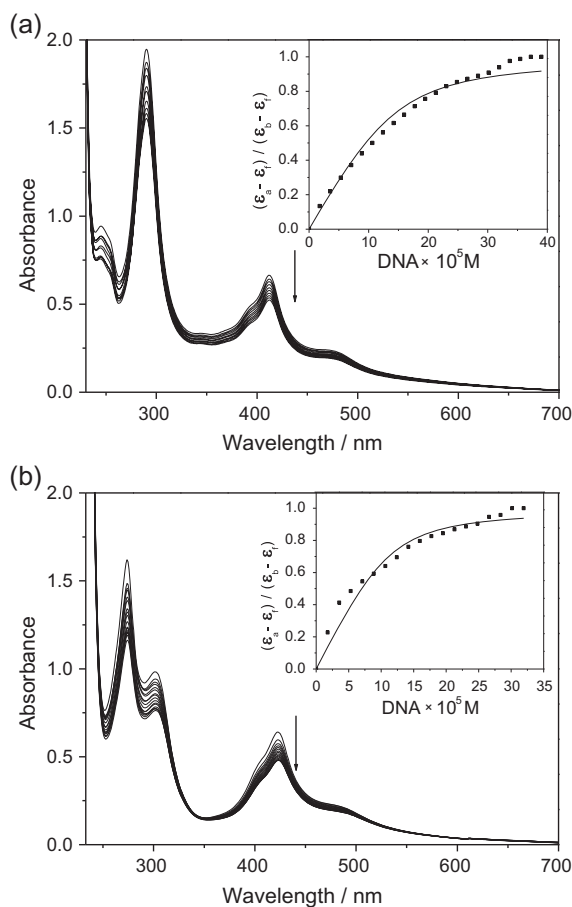
Figure 1. UV–vis spectra of **1** (a) and **2** (b) in buffer A upon addition of CT-DNA, [Ru] = 20 μM, [DNA] = 0–400 μM. Arrow shows the absorbance change upon increasing DNA concentration. Inset: plots of $(\varepsilon_a - \varepsilon_f)/(\varepsilon_b - \varepsilon_f)$ vs. [DNA] for the titration of DNA to Ru(II) complexes.

In order to further evaluate quantitatively the DNA binding affinities of the two complexes, the intrinsic binding constants K_b were obtained by monitoring the changes of the π–π* transition at 412 nm for **1** and at 413 nm for **2** using equations (1a) and (1b) [61]. The values of K_b are $(2.4 \pm 0.2) \times 10^5$ M^{-1} ($s = 3.26$) and $(4.0 \pm 0.6) \times 10^5$ M^{-1} ($s = 2.81$) for **1** and **2**, respectively. The K_b values are much smaller than those of similar Ru(II) complexes with asymmetric ligands, [Ru(bpy)$_2$pidbp]$^{2+}$ (1.68×10^6 M^{-1}) and Ru(phen)$_2$pidbp]$^{2+}$ (3.09×10^6 M^{-1}) [48]. This may be due to the reduced aromatic planarity of the pipz ligand. The above results demonstrate that the two complexes bind to DNA with high affinities, and the DNA-binding affinity of **2** is stronger than **1** due to the size of the planar aromatic ligand and hydrophobicity of the ancillary ligands.

3.2. Steady-state emission studies

Emission titration experiments are also one of the most commonly used methods to investigate the interaction between complexes and DNA, and can provide important information

for DNA-binding mode. Changes in the emission spectra of **1** and **2** with increasing CT-DNA concentration are shown in figure 2. Upon excitation at 450 nm, in the absence of DNA, **1** emits negligible background fluorescence in buffer A at ambient temperature while **2** is weakly fluorescent with maximum fluorescence at 586 nm. Upon addition of CT-DNA, the fluorescence emission intensity increases by a factor of 4.9 for **1** and by a factor of 4.5 for **2** (figure 2). The emission enhancement in the presence of DNA may be due to the protection of the phenazine nitrogens from solvent molecules. Other ruthenium(II) complexes possessing a phenazine-based ligand which act as light switches upon binding to DNA have been reported previously, such as $[Ru(bpy)_2(dppz)]^{2+}$, $[Ru(bpy)_2(tpphz)]^{2+}$, and $[Ru(bpy)_2(pidbp)]^{2+}$ [14, 45, 46, 48]. The fluorescence emission of these complexes was enhanced upon DNA intercalation, functioning as DNA "molecular light switches." Their "light switch" effects are attributed to hydrogen bond formation between the phenazine unit of the complexes and water in the absence of DNA, which quenches the excited state emission. However, although the fluorescence intensity of two Ru(II) complexes reported in this study is enhanced in the presence of DNA, the emission is weak, making them unsuitable DNA "light switch" complexes. Other Ru(II) complexes incorporating asymmetric ligands have also been found to be weakly fluorescent [25, 48]. The fluorescence titration results suggested that the two complexes strongly interact with DNA and are protected from solvent by DNA. The hydrophobic environment inside the DNA helix reduces the accessibility of solvent water to the complex and the complex mobility is restricted at the binding site, leading to a decrease in vibration modes associated with relaxation.

EB competitive binding experiments were carried out using either **1** or **2** as a fluorescence quencher. EB is strongly fluorescent in the presence of CT-DNA due to its strong intercalation between the adjacent DNA base pairs. The fluorescence of the DNA–EB system can be quenched by addition of a second compound, which displaces the intercalating EB. The fluorescence quenching efficiency of the DNA–EB system in the presence of
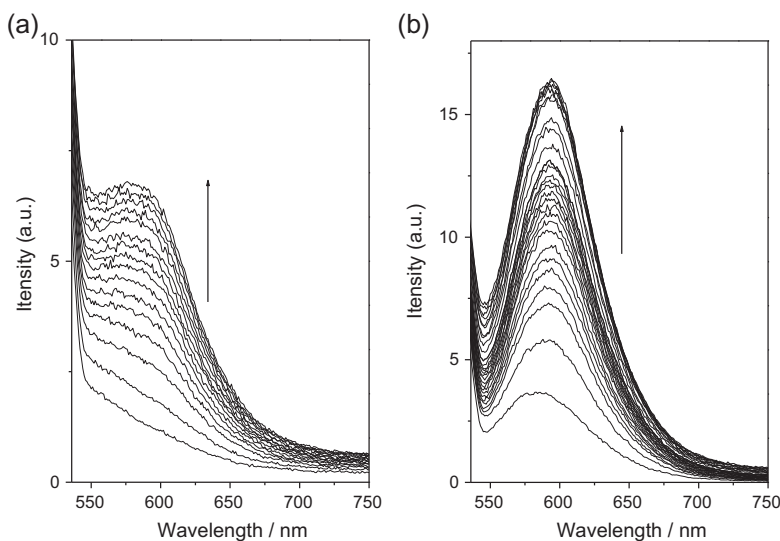

Figure 2. Fluorescence spectra of Ru(II) complexes (5 μM) **1** (a) and **2** (b) in buffer A at 298 K in the absence and presence of CT-DNA. Arrow shows the intensity change upon increasing DNA concentration.

another compound is typically used to evaluate the DNA binding affinities of these species. Upon excitation at 515 nm, the two Ru(II) complexes and the DNA-bound Ru(II) complexes emit negligible fluorescence; therefore, their emission is insignificant in the EB competitive binding experiment. Fluorescence quenching spectra of DNA-bound EB by the Ru(II) complexes are shown in figure 3. Addition of the complexes to the DNA–EB system resulted in obvious decrease in EB emission intensities, which indicates that the EB molecules were displaced from the DNA–EB system by **1** or **2**. However, addition of excess Ru (II) complexes could not quench the emission of the DNA–EB system, which suggests that both complexes bind to DNA with lower affinities than EB. From the plot of percentage of quenching fluorescence, $(I_0 - I)/I_0$ *versus* [Ru]/[EB], 50% of the EB molecules were displaced from the DNA–EB system by the Ru complex at concentration ratios of [Ru]/[EB] $= 15.9 \pm 0.2$ for **1** and 10.7 ± 0.1 for **2**, respectively. Using a DNA-binding constant of $1.4 \times 10^6\,M^{-1}$ for EB [64, 65], the apparent DNA binding constants K_{app} of the two complexes were calculated using equation (3) [66],
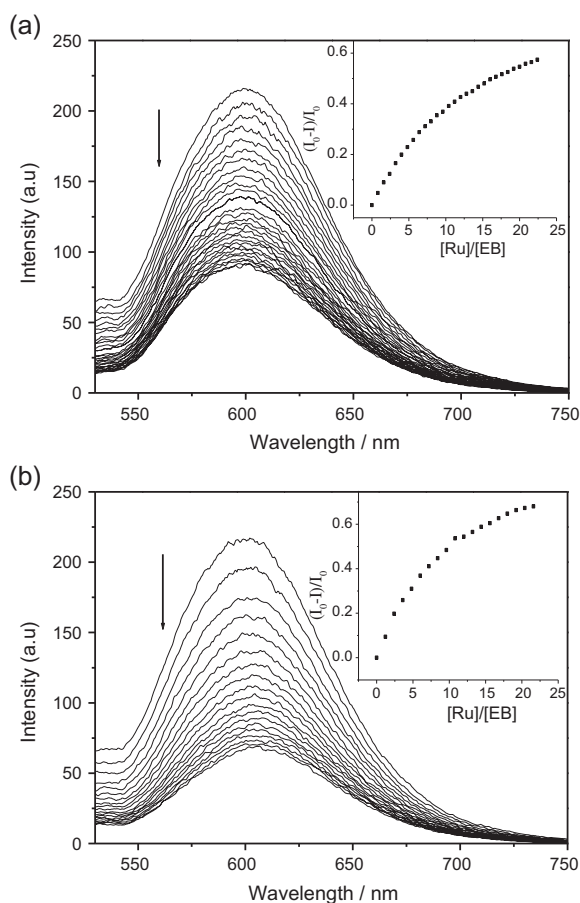

Figure 3. Changes in fluorescence spectra of DNA–EB system in buffer A with increasing concentration of **1** (a) and **2** (b), [DNA] = 100 μM, [EB] = 5 μM. Arrow shows the intensity change upon increasing complex concentrations. Inset: plots of $(I_0 - I)/I_0$ *vs.* [Ru]/[EB].

$$K_{app} = K_{EB} \ ([EB]_{50\%}/[Ru]_{50\%}) \tag{3}$$

where K_{app} is the apparent DNA binding constant for the Ru(II) complex, K_{EB} is the DNA-binding constant of EB, and $[EB]_{50\%}$ and $[Ru]_{50\%}$ are the EB and Ru(II) complex concentrations at 50% fluorescence, respectively. $K_{app} = (8.81 \pm 0.09) \times 10^4 \ M^{-1}$ for **1** and $(1.30 \pm 0.02) \times 10^5 \ M^{-1}$ for **2**, respectively, which is slightly smaller than the K_b values derived from the absorption spectral studies. The results also showed that **2** exhibits stronger DNA-binding affinity than **1**.

3.3. *Viscosity properties*

To further clarify the DNA-binding mode of both complexes, DNA viscosity measurements were carried out on CT-DNA with increasing concentrations of the Ru(II) complexes. DNA viscosity measurements are a useful means of determining whether a complex intercalates with DNA, and is sensitive to change in the length of the DNA strand (i.e. viscosity and sedimentation) and is regarded as the least ambiguous and most important method to probe the DNA-binding mode in the absence of crystallographic structural data [67, 68]. Classical intercalation demands that the DNA helix lengthens as base pairs are separated to accommodate the bound ligand, which leads to an increase in DNA viscosity. However, a partial, non-classical intercalation of complex could reduce the effective length of DNA by bending (or kinking) of the DNA helix, which results in a reduction of the DNA viscosity [69]. In addition, some complexes which interact with DNA by an electrostatic-binding mode have little effect on DNA viscosity.
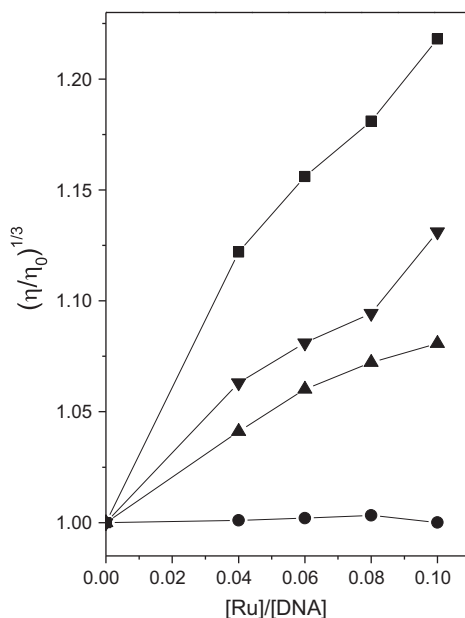

Figure 4. Effects of the increase in amounts of EB (■), **1** (▲) and **2** (▼) and $[Ru(bpy)_3]^{2+}$ (●) on the relative viscosity of CT-DNA at 30 ($\pm$0.1) °C. The total concentration of DNA is 0.25 mM.

The effect of addition of EB, **1**, **2**, and $[Ru(bpy)_3]^{2+}$ on the CT-DNA viscosity is shown in figure 4. Addition of the well-known intercalator EB results in a strong increase in the DNA viscosity and lengthens the DNA double helix by intercalation into the DNA base pairs, while $[Ru(bpy)_3]^{2+}$, which binds to DNA via an electrostatic-binding mode, has little effect on DNA viscosity. Upon increasing the concentrations of either **1** or **2**, the relative viscosity of CT-DNA increases steadily, similar to the behavior observed with EB. The viscosity, which may depend on the DNA-binding mode and affinity, follows the order $EB > 2 > 1 > [Ru(bpy)_3]^{2+}$. This result suggests that the two complexes can bind to DNA through a classical intercalative binding mode. The difference in the binding strength between **1** and **2** may be due to the more hydrophobic nature of the ancillary ligand phen, and **2** inserting further between the DNA base pairs and thus showing a larger DNA-binding affinity compared with **1**. The experimental results are consistent with the above spectroscopic results.

3.4. Photocleavage of pBR 322 DNA by the Ru(II) complexes

PDT agents usually use a photosensitizer of molecular oxygen by generating singlet oxygen or hydroxyl radicals, which leads to cell death. Many Ru(II) complexes with polypyridyl ligands cleave DNA upon irradiation and have been investigated for their potential use in PDT [16–18]. The majority of them, commonly known as "DNA photocleavers," are activated by light and generate singlet oxygen, thus inducing single-strand or double-strand cleavage of DNA. Upon irradiation, DNA cleavage is attributed to the well-behaved redox and photochemical properties of the ruthenium complexes. The DNA photocleavge activity of the present complexes was studied by gel electrophoresis using supercoiled pBR322 DNA in TBE buffer (pH 7.8). In general, when circular plasmid DNA is subjected to gel electrophoresis, relatively fast migration will be observed for the intact supercoiled form (Form I). If scission occurs on one strand (nicked circulars), the supercoil will relax to generate a slower moving nicked circular form (Form II). If both strands are cleaved, a linear form (Form III) that migrates between Forms I and II will be generated [70].

Figure 5 shows the results for the gel electrophoresis separation of pBR322 DNA after incubation with varying concentrations of the Ru(II) complexes under irradiation at 365 nm. A control experiment using DNA alone does not show any obvious DNA cleavage (figure 5: lane 0). Both complexes exhibit efficient DNA photocleavage activity as evidenced by the conversion of supercoiled to the nicked circular form of DNA. Figure 5 shows that the cleavage reaction is strictly dependent on complex concentration. Upon increasing the concentration of **1** [figure 5(a)] and **2** [figure 5(b)], the amount of Form I is decreased, whereas that of Form II is increased. Notably, under the same experimental conditions, when the concentration reached 60 μM, **2** promotes almost complete conversion
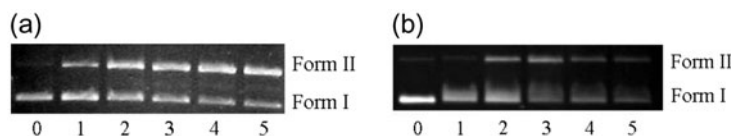

Figure 5.   The agarose gel electrophoresis pattern of supercoiled pBR322 plasmid DNA upon irradiation (365 nm) for 80 min in the presence of Ru(II) complexes. Lane 0, DNA alone; lane 1, DNA + Ru (20 μM) in the dark; lanes 2–5: **1** (a) at 20, 40, 80, and 120 μM and **2** (b) at 10, 20, 40, and 60 μM.
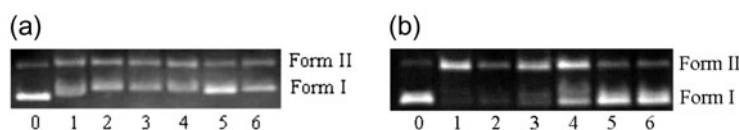
Figure 6. Agarose gel showing cleavage of pBR322 DNA incubated with **1** (80 μM) (a), **2** (80 μM) (b) and different inhibitors after 80 min irradiation at 365 nm. Lane 0: DNA alone, lane 1: DNA + Ru, lanes 2–6: DNA + Ru + 1 M DMSO, 100 mM mannitol, 1000 U mL^{-1} SOD, 25 mM NaN$_3$, 1.2 mM histidine.

of DNA from Form I to Form II. The DNA cleavage results show that both **1** and **2** can cleave DNA upon irradiation and **2** exhibits a higher efficiency for DNA photocleavage than **1**, which may be attributed to its higher DNA-binding affinity.

To further explore the nature of the reactive oxygen species responsible for DNA photocleavage of the two Ru(II) complexes, experiments were performed in the presence of the hydroxyl radical (OH$^{\cdot}$) scavengers DMSO and mannitol [59, 60, 62], the singlet oxygen ($^1O_2$) scavengers NaN$_3$ and histidine [60], and a superoxide anion radical ($O_2^{\cdot-}$) scavenger, superoxide dismutase (SOD). As shown in figure 6, the presence of DMSO, mannitol or SOD did not affect the cleavage activity of the two complexes, suggesting that OH$^{\cdot}$ and $O_2^{\cdot-}$ are not involved in the DNA photocleavage reaction. However, the presence of NaN$_3$ and histidine (lanes 5 and 6) led to strong inhibition of the DNA cleavage activity, which suggests that $^1O_2$ is likely to be the cleaving agent; hence, the mechanism of DNA cleavage is an oxidative process via singlet oxygen generation.

In order to further explore the $^1O_2$ generation abilities of **1** and **2**, chemical trapping experiments were conducted to determine the quantum yields of $^1O_2$ generation. DPBF reacts with singlet oxygen generated by the Ru(II) complexes, leading to a decrease in fluorescence. Fluorescence spectra for DPBF in the presence of Ru(II) complexes irradiated at 450 nm are shown in figure 7. Using [Ru(bpy)$_3$]$^{2+}$ as a standard ($\Phi_\Delta^S = 0.81$ [71]), Φ_Δ for **1** and **2** in CH$_3$OH were calculated using equations (2a) and (2b) and determined to be 0.63 and 0.71, respectively. The order of the Φ_Δ values for these complexes are [Ru(bpy)$_3$]$^{2+}$ > **2** > **1**. These results reveal that the two Ru(II) complexes exhibit a higher singlet oxygen generation rate than [Ru(bpy)$_3$]$^{2+}$. This may explain their high efficiency with respect to DNA photocleavage.

3.5. *Topoisomerase I inhibition by Ru(II) complexes*

DNA topoisomerase I (Topo I), an important nuclear enzyme, catalyzes the relaxation of supercoiled DNA, knot or unknot single-stranded circular DNA and can form double-strand circular DNA from two single-stranded DNA rings. DNA relaxation experiments were carried out to determine the influence of the ruthenium(II) complexes on Topo I activities by incubating supercoiled pBR322 DNA, Topo I and varying concentrations of the Ru(II) complexes. DNA topoisomerase I inhibitory activities of the two complexes are shown in figure 8. In the absence of the Ru(II) complexes, Topo I can completely relax supercoiled DNA. However, after incubation with the Ru(II) complexes, the ability of Topo I to relax negatively supercoiled plasmid DNA was reduced. To determine the IC$_{50}$ values of the two Ru(II) complexes, the concentration-dependent Topo I inhibition assays of both complexes were carried out. With increasing concentration of Ru(II) complex, the amount of supercoiled DNA increases. The IC$_{50}$ is ~80 μM for **1** and ~60 μM for **2**. Although the
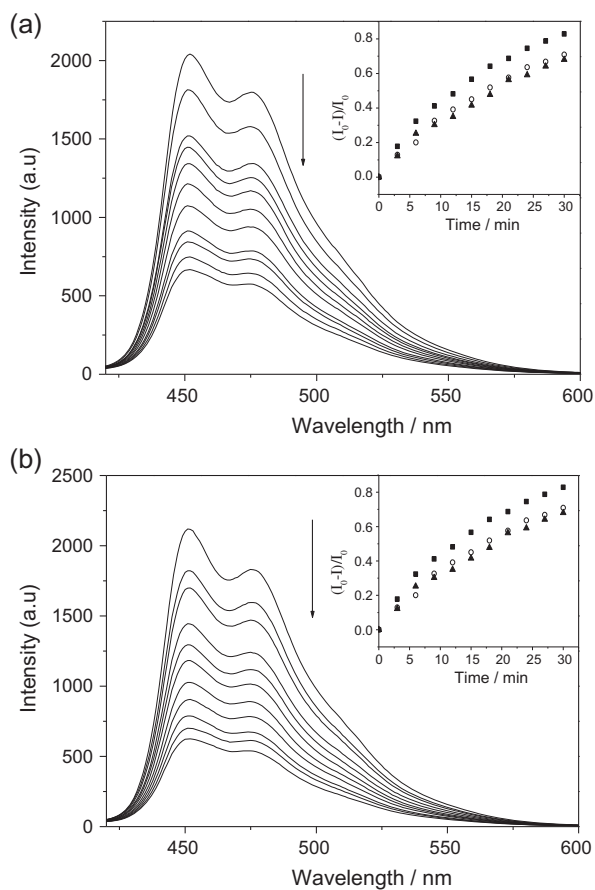
Figure 7. Emission spectra changes of the DPBF in the presence of **1** (a) and **2** (b) upon irradiation at 450 nm. Inset: the DPBF consumption percentage as a function of irradiation time in air-equilibrated CH_3OH solution of $[Ru(bpy)_3]^{2+}$ (■), **1** (▲) and **2** (○).
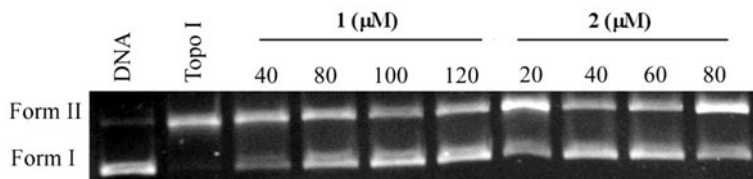

Figure 8. Effects of different concentrations of **1** and **2** on the activity of DNA Topo I.

IC_{50} values are larger than the IC_{50} value of other Topo I inhibitors [19–25, 55, 56], both complexes still exhibited obvious Topo I inhibitory activity. The above results suggest that the two Ru(II) complexes block the DNA strand passage event for this enzyme, acting as catalytic inhibitors of Topo I.
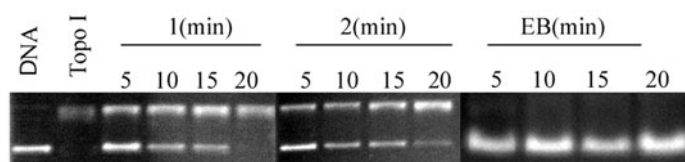
Figure 9.   The time dependence of Topo I DNA strand passage assays in the presence of **1**, **2**, and EB.

As reported before, intercalative agents can interfere with the DNA relaxation reaction by inhibiting Topo I catalysis or by altering the apparent topological state of DNA, with both resulting in inhibition of the enzyme. In order to determine which is responsible for the Topo I inhibitory activity of two Ru(II) complexes, DNA strand passage assays were performed. The effects of the Ru(II) complexes on enzyme-catalyzed DNA strand passage were assessed by comparing the rate of relaxation of negatively supercoiled plasmid in the absence of drug to the rate of supercoiling of relaxed plasmid in the presence of 80 μM Ru (II) complex or EB. As shown in figure 9, clear changes of the rate of supercoiling relaxation in the presence of the Ru(II) complexes were observed. The rate of Topo I-catalyzed DNA relaxation in the presence of the Ru(II) complexes were lower than the rate for EB. These findings indicate that Ru(II) complexes are catalytic inhibitors of Topo I.

4. Conclusion

Two new Ru(II) complexes, $[Ru(bpy)_2(pipz)]^{2+}$ (**1**) and $[Ru(phen)_2(pipz)]^{2+}$ (**2**), have been synthesized and characterized. The DNA binding properties were examined by various methods. The results support both complexes interacting with DNA via intercalation. Both complexes were also found to be efficient DNA photocleavers and **2** exhibits a stronger DNA photocleavage efficiency compared with **1**. The mechanistic studies revealed that singlet oxygen most likely plays an important role in the DNA-induced photocleavage by the two Ru(II) complexes. The results of topoisomerase I inhibition experiments suggest that both complexes are catalytic inhibitors of Topo I.

Supplementary material

The supplementary material for this paper is available online at http://dx.doi.10.1080/00958972.2015.1057132.

Disclosure statement

No potential conflict of interest was reported by the authors.

Funding

References

[1] K.W. Kohn. *Cancer Res.*, **56**, 5533 (1996).
[2] B. Lippert. *Cisplatin: Chemistry and Biochemistry of A Leading Anti-cancer Drug*, Wiley-VCH, Weinheim (1999).
[3] J. Reedijk. *Chem. Commun.*, 801, (1996).
[4] Z.J. Guo, P.J. Sadler. *Adv. Inorg. Chem.*, **49**, 183 (2000).
[5] J.D. Roberts, J. Peroutka, N. Farrell. *J. Inorg. Biochem.*, **77**, 51 (1999).
[6] D.S. Pilch, M.A. Kirolos, X.Y. Liu, G.E. Plum, K.J. Breslauer. *Biochemistry*, **34**, 9962 (1995).
[7] P. Mustonen, P.K.J. Kinnunen. *J. Biol. Chem.*, **268**, 1074 (1993).
[8] S.S. Bhat, A.S. Kumbhar, P. Lönnecke, E. Hey-Hawkins. *Inorg. Chem.*, **49**, 4843 (2010).
[9] B. Sun, J.X. Guan, L. Xu, B.L. Yu, L. Jiang, J.F. Kou, L. Wang, X.D. Ding, H. Chao, L.N. Ji. *Inorg. Chem.*, **48**, 4637 (2009).
[10] B.M. Zeglis, V.C. Pierre, J.K. Barton. *Chem. Commun.*, 4565 (2007).
[11] E. Rüba, J.R. Hart, J.K. Barton. *Inorg. Chem.*, **43**, 4570 (2004).
[12] Y.Z. Ma, H.J. Yin, K.Z. Wang. *J. Phys. Chem.*, **113**, 11039 (2009).
[13] J.C. Genereux, J.K. Barton. *Chem. Rev.*, **110**, 1642 (2010).
[14] R.M. Hartshorn, J.K. Barton. *J. Am. Chem. Soc.*, **114**, 5919 (1992).
[15] A. Sassolas, B.D. Leca-Bouvier, L.J. Blum. *Chem. Rev.*, **108**, 109 (2008).
[16] Y.J. Sun, L.E. Joyce, N.M. Dickson, C. Turro. *Chem. Commun.*, **46**, 6759 (2013).
[17] C.T. Poon, P.S. Chan, C. Man, F.L. Jiang, R.N.S. Wong, N.K. Mak, D.W.J. Kwong, S.W. Tsao, W.K. Wong. *J. Inorg. Biochem.*, **104**, 62 (2010).
[18] E. Wachter, D.K. Heidary, B.S. Howerton, S. Parkin, E.C. Glazer. *Chem. Commun.*, **48**, 9649 (2012).
[19] J.F. Kou, C. Qian, J.Q. Wang, X. Chen, L.L. Wang, H. Chao, L.N. Ji. *J. Biol. Inorg. Chem.*, **17**, 81 (2012).
[20] K.J. Du, J.Q. Wang, J.F. Kou, G.Y. Li, L.L. Wang, H. Chao, L.N. Ji. *Eur. J. Med. Chem.*, **46**, 1056 (2011).
[21] K.J. Du, J.W. Liang, Y. Wang, J.F. Kou, C. Qian, L.N. Ji, H. Chao. *Dalton Trans.*, **43**, 17303 (2014).
[22] Y.C. Wang, C. Qian, Z.L. Peng, X.J. Hou, L.L. Wang, H. Chao, L.N. Ji. *J. Inorg. Biochem.*, **130**, 15 (2014).
[23] H.Y. Huang, P.Y. Zhang, H.M. Chen, L.N. Ji, H. Chao. *Chem. - A Eur. J.*, **21**, 715 (2015).
[24] H.Y. Huang, P.Y. Zhang, B.L. Yu, Y. Chen, J.Q. Wang, L.N. Ji, H. Chao. *J. Med. Chem.*, **57**, 8971 (2014).
[25] X.W. Liu, S.B. Zhang, L. Li, Y.D. Chen, J.L. Lu. *J. Organomet. Chem.*, **729**, 1 (2013).
[26] Y.Y. Xie, H.L. Huang, J.H. Yao, G.J. Lin, G.B. Jiang, Y.J. Liu. *Eur. J. Med. Chem.*, **63**, 603 (2013).
[27] Y.Y. Xie, Z.Z. Li, G.J. Lin, H.L. Huang, X.Z. Wang, Z.H. Liang, G.B. Jiang, Y.J. Liu. *Inorg. Chim. Acta*, **405**, 228 (2013).
[28] G.B. Jiang, J.H. Yao, J. Wang, W. Li, B.J. Han, Y.Y. Xie, G.J. Lin, H.L. Huang, Y.J. Liu. *New J. Chem.*, **38**, 2554 (2014).
[29] W. Li, G.B. Jiang, J.H. Yao, X.Z. Wang, J. Wang, B.J. Han, Y.Y. Xie, G.J. Lin, H.L. Huang, Y.J. Liu. *J. Photochem. Photobiol., B*, **140**, 94 (2014).
[30] Y.J. Liu, C.H. Zeng, Z.H. Liang, J.H. Yao, H.L. Huang, Z.Z. Li, F.H. Wu. *Eur. J. Med. Chem.*, **45**, 3087 (2010).
[31] Y.J. Liu, C.H. Zeng, H.L. Huang, L.X. He, F.H. Wu. *Eur. J. Med. Chem.*, **45**, 564 (2010).
[32] M.J.E. Clark. *Ruthenium and Other Metal Complexes in Cancer Chemotherapy*, Springer-Verlag, Heidelberg (1989).
[33] C.D. Fan, Q. Wu, T.F. Chen, Y.B. Zhang, W.J. Zheng, Q. Wang, W.J. Mei. *Med. Chem. Commun.*, **5**, 597 (2014).
[34] R. Fernández, M. Melchart, A. Habtemariam, S. Parsons, P.J. Sadler. *Chem. - A Eur. J.*, **10**, 5173 (2004).
[35] A. Levina, A. Mitra, P.A. Lay. *Metallomics*, **1**, 458 (2009).
[36] M.R. Gill, J.A. Thomas. *Chem. Soc. Rev.*, **41**, 3179 (2012).
[37] J.L. Yao, X. Gao, W.L. Sun, X.Z. Fan, S. Shi, T.M. Yao. *Inorg. Chem.*, **51**, 12591 (2012).
[38] E. Baggaley, M.R. Gill, N.H. Green, D. Turton, I.V. Sazanovich, S.W. Botchway, C. Smythe, J.W. Haycock, J.A. Weinstein, J.A. Thomas. *Angew. Chem. Int. Ed.*, **53**, 3367 (2014).
[39] M.R. Gill, J. Garcia-Lara, S.J. Foster, C. Smythe, G. Battaglia, J.A. Thomas. *Nat. Chem.*, **1**, 662 (2009).
[40] A.E. Friedman, J.C. Chambron, J.P. Sauvage, N.J. Turro, J.K. Barton. *J. Am. Chem. Soc.*, **112**, 4960 (1990).
[41] L.S. Ling, Z.H. He, G.W. Song, Y.E. Zeng, C. Wang, C.L. Bai, X.D. Chen, P. Shen. *Anal. Chim. Acta*, **436**, 207 (2001).
[42] L.S. Ling, Z.K. He, F. Chen, Y.-E. Zeng. *Talanta*, **59**, 269 (2003).
[43] A.P. de Silva, N.D. McClenaghan. *Chem. - A Eur. J.*, **10**, 574 (2004).
[44] Y. Jiang, X. Fang, C. Bai. *Anal. Chem.*, **76**, 5230 (2004).

[45] Y. Liu, A. Chouai, N.N. Degtyareva, D.A. Lutterman, K.R. Dunbar, C. Turro. *J. Am. Chem. Soc.*, **127**, 10796 (2005).
[46] A.T. Steven, K. Roni, S. Dietrich. *Inorg. Chem.*, **38**, 5196 (1999).
[47] J.L. Yao, X. Gao, W.L. Sun, X.Z. Fan, S. Shi, T.M. Yao. *Inorg. Chem.*, **51**, 12591 (2012).
[48] X.W. Liu, Y.D. Chen, L. Li, J.L. Lu, D.S. Zhang. *Spectrochim. Acta, Part A*, **86**, 554 (2012).
[49] J. Sun, W.X. Chen, X.D. Song, X.H. Zhao, A.Q. Ma, J.X. Chen. *J. Coord. Chem.*, **68**, 308 (2015).
[50] P. Zhao, J. Li, L.J. Yang, J.Z. Lu, H.M. Guo, L.N. Ma, B.H. Ou. *J. Coord. Chem.*, **66**, 4220 (2013).
[51] S. Selvamurugan, P. Viswanathamurthi, A. Endo, T. Hashimoto, K. Natarajan. *J. Coord. Chem.*, **66**, 4052 (2013).
[52] J.C. Wang. *Annu. Rev. Biochem.*, **65**, 635 (1996).
[53] J.M. Berger, S.J. Gamblin, S.C. Harrison, J.C. Wang. *Nature*, **379**, 225 (1996).
[54] J.C. Wang. *Nat. Rev. Mol. Cell Biol.*, **3**, 430 (2002).
[55] F. Gao, H. Chao, J.Q. Wang, Y.X. Yuan, B. Sun, Y.F. Wei, B. Peng, L.N. Ji. *J. Biol. Inorg. Chem.*, **12**, 1015 (2007).
[56] X.J. He, L.H. Jin, L.F. Tan. *Spectrochim. Acta, Part A*, **135**, 101 (2015).
[57] B.P. Sullivan, D.J. Salmon, T.J. Meyer. *Inorg. Chem.*, **17**, 3334 (1978).
[58] B.B. Shi, Y.M. Zhang, T.B. Wei, P. Zhang, Q. Lin, H. Yao. *New J. Chem.*, **37**, 3737 (2013).
[59] J. Bolger, A. Gourdon, E. Ishow, J.P. Launay. *Inorg. Chem.*, **35**, 2937 (1996).
[60] E. Ishow, A. Gourdon, J.P. Launay. *Chem. Commun.*, 1909 (1998).
[61] J.D. McGhee, P.H. von Hippel. *J. Mol. Biol.*, **86**, 469 (1974).
[62] G. Cohen, H. Eisenberg. *Biopolymers*, **8**, 45 (1969).
[63] M.K. Brennaman, T.J. Meyer, J.M. Papanikolas. *J. Phys. Chem.*, **108**, 9938 (2004).
[64] M.J. Waring. *J. Mol. Biol.*, **13**, 269 (1965).
[65] J.B. Lepecq, C. Paoletti. *J. Mol. Biol.*, **27**, 87 (1967).
[66] D.L. Boger, B.E. Fink, S.R. Brunette, W.C. Tse, M.P. Hedrick. *J. Am. Chem. Soc.*, **123**, 5878 (2001).
[67] S. Satyanarayana, J.C. Dabrowiak, J.B. Chaires. *Biochemistry*, **31**, 9319 (1992).
[68] S. Satyanarayana, J.C. Dabrowiak, J.B. Chaires. *Biochemistry*, **32**, 2573 (1993).
[69] J.K. Barton, J.M. Goldberg, C.V. Kumar, N.J. Turro. *J. Am. Chem. Soc.*, **108**, 2081 (1986).
[70] J.K. Barton, A.L. Raphael. *J. Am. Chem. Soc.*, **106**, 2466 (1984).
[71] A.A. Abdel-Shafi, P.D. Beer, R.J. Mortimer, F. Wilkinson. *J. Phys. Chem.*, **104**, 192 (2000).